

POD-based reduced-order model of an eddy-current levitation problem

MD Rokibul Hasan, Laurent Montier, Thomas Henneron, and Ruth V. Sabariego

Abstract The accurate and efficient treatment of eddy-current problems with movement is still a challenge. Very few works applying reduced-order models are available in the literature. In this paper, we propose a proper-orthogonal-decomposition reduced-order model to handle these kind of motional problems. A classical magnetodynamic finite element formulation based on the magnetic vector potential is used as reference and to build up the reduced models. Two approaches are proposed. The TEAM workshop problem 28 is chosen as a test case for validation. Results are compared in terms of accuracy and computational cost.

1 Introduction

The finite element (FE) method is widely used and versatile for accurately modelling electromagnetic devices accounting for eddy current effects, non-linearities, movement,... However, the FE discretization may result in a large number of unknowns, which maybe extremely expensive in terms of computational time and memory. Furthermore, the modelling of a movement requires either remeshing or ad-hoc techniques. Without being exhaustive, it is worth mentioning: the hybrid finite-element boundary-element (FE-BE) approaches [1], the sliding mesh techniques (rotating machines) [2] or the mortar FE approaches [3].

Physically-based reduced models are the most popular approaches for efficiently handling these issues. They extract physical parameters (inductances, flux linkages,...) either from simulations or measurements and construct look-up tables cov-

MD Rokibul Hasan · Ruth V. Sabariego
KU Leuven, Dept. Electrical Engineering (ESAT), Leuven & EnergyVille, Genk, Belgium, e-mail: rokib.hasan@esat.kuleuven.be, ruth.sabariego@esat.kuleuven.be

Laurent Montier · Thomas Henneron
Laboratoire d'Electrotechnique et d'Electronique de Puissance, Arts et Metiers ParisTech, Lille, France, e-mail: laurent.montier@ensam.eu, thomas.henneron@univ-lille1.fr

ering the operating range of the device at hand [4, 5]. Future simulations are performed by simple interpolation, drastically reducing thus the computational cost. However, these methods depend highly on the expert’s knowledge to choose and extract the most suitable parameters.

Mathematically-based reduced-order (RO) techniques are a feasible alternative, which are gaining interest in electromagnetism [6]. RO modelling of static coupled system has already been implemented in [7, 8]. Few RO works have addressed problems with movement (actuators, electrical machines, etc.) [9–11].

In [9], authors consider a POD-based FE-BE model electromagnetic device comprising nonlinear materials and movement. Meshing issues are avoided but the system matrix is not sparse any more, increasing considerably the cost of generating the RO model. In [10], a magnetostatic POD-RO model of a permanent magnet synchronous machine is studied. A locked step approach is used, so the mesh and associated number of unknowns remains constant. A POD-based block-RO model is proposed in [11, 12], where the domain is split in linear and nonlinear regions and the ROM is applied only to the linear part.

In this paper, we consider a POD-based FE model of a levitation problem, namely the Team Workshop problem 28 (TWP28) [5, 13] (a conducting plate above two concentric coils, see Fig. 1). The movement is modelled with two RO models based on: 1) FE with automatic remeshing of the complete domain; 2) FE with constraint remeshing, i.e., localized deformation of the mesh around the moving plate, hereafter referred to as mesh deformation. Both models are validated in the time domain and compared in terms of computational efficiency.

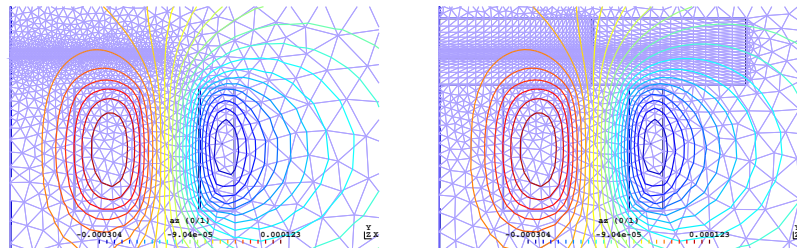


Fig. 1: 2D axisymmetric mesh of TWP28: aluminium plate above two concentric coils (12.8 mm clearance). Real part of the magnetic flux density. Left: automatic remeshing of the full domain, Right: mesh deformation of sub-domain around plate with nodes fixed at it’s boundaries (except axes).

2 Magnetodynamic levitation model

Let us consider a bounded domain $\Omega = \Omega_c \cup \Omega_c^C \in \mathbb{R}^3$ with boundary Γ . The conducting and non-conducting parts of Ω are denoted by Ω_c and Ω_c^C , respectively. The (modified) magnetic-vector-potential (a -) magnetodynamic formulation (weak form of Ampère's law) reads: find a , such that

$$(\nu \operatorname{curl} a, \operatorname{curl} a')_{\Omega} + (\sigma \partial_t a, a')_{\Omega_c} + \langle \hat{n} \times h, a' \rangle_{\Gamma} = (j_s, a')_{\Omega_s}, \forall a' \quad (1)$$

with a' test functions in a suitable function space; $b(t) = \operatorname{curl} a(t)$, the magnetic flux density; $j_s(t)$ a prescribed current density and \hat{n} the outward unit normal vector on Γ . Volume integrals in Ω and surface integrals on Γ of the scalar product of their arguments are denoted by $(\cdot, \cdot)_{\Omega}$ and $\langle \cdot, \cdot \rangle_{\Omega}$. The derivative with respect to time is denoted by ∂_t . We further assume linear isotropic and time independent materials with magnetic constitutive law, so that the magnetic field is $h(t) = \nu b(t)$ (reluctivity ν) and electric constitutive law, given by induced eddy current density $j(t) = \sigma e(t)$, (conductivity σ) where, electric field $e(t) = -\partial_t a(t)$. Assuming a rigid Ω_c (no deformation) and a purely translational movement (no rotation, no tilting), the electromagnetic force appearing due to the eddy currents in Ω_c can be modelled as a global quantity with only one component (vertical to the plate). If Ω_c is non-magnetic, Lorentz force can be used:

$$F_{em}(t) = \int_{\Omega_c} j(t) \times b(t) \, d\Omega_c = \int_{\Omega_c} -\sigma \partial_t a(t) \times \operatorname{curl} a(t) \, d\Omega_c. \quad (2)$$

The 1D mechanical equation governing the above described levitation problem reads:

$$m \partial_t v(t) + \xi v(t) + ky(t) + mg = F_{em}(t) \quad (3)$$

where unknown $y(t)$ is the center position of the moving body in the vertical direction, $v(t) = \partial_t y(t)$ is the velocity of the moving body, m is the mass of the moving body, g is the acceleration of gravity, ξ is the scalar viscous friction coefficient, k is the elastic constant. We apply the backward Euler method to solve (3). The moving body displacement of system (3) results from the ensuing electromagnetic force generated by system (1) and thus affects the geometry. Given that, the dynamics of the mechanical equation is much slower than the electromagnetic equation, if the time-step is taken sufficiently small, one can decouple the equations. Under this condition, the electromagnetic and mechanical equations can be solved alternatively rather than simultaneously by the weak electromechanical coupling algorithm of [14]. We adopt this approach.

3 POD-based model order reduction

The proper orthogonal decomposition (POD) is applied to reduce the matrix system resulting from the FE discretisation of (1):

$$A\partial_t x(t) + Bx(t) = C(t). \quad (4)$$

where $x(t) \in \mathbb{R}^{N \times 1}$ is the time-dependent column vector of N unknowns, $A, B \in \mathbb{R}^{N \times N}$ are the matrices of coefficients and $C(t) \in \mathbb{R}^{N \times 1}$ is the source column vector. Furthermore, the system (4) is discretized in time by means of the backward Euler scheme. A system of algebraic equation is obtained for each time step from t_{k-1} to $t_k = t_{k-1} + \Delta t$, Δt the step size. The discretized system reads:

$$[A_{\Delta t} + B]x_k = A_{\Delta t}x_{k-1} + C_k \quad (5)$$

with $A_{\Delta t} = \frac{A}{\Delta t}$, $x_k = x(t_k)$ the solution at instant t_k , $x_{k-1} = x(t_{k-1})$ the solution at instant t_{k-1} , C_k the right-hand side at instant t_k .

In RO techniques, the solution vector $x(t)$ is approximated by a vector $x^r(t) \in \mathbb{R}^{M \times 1}$ within a reduced subspace spanned by $\Psi \in \mathbb{R}^{N \times M}$, $M \ll N$,

$$x(t) \approx \Psi x^r(t), \quad (6)$$

with Ψ an orthonormal projection operator generated from the time-domain full solution $x(t)$ via snapshot techniques [15].

Let us consider the snapshot matrix, $S = [x_1, x_2, \dots, x_M] \in \mathbb{R}^{N \times M}$ from the set of solution x_k for the selected number of time steps. Applying the singular value decomposition (SVD) to S as,

$$S = \mathcal{U} \Sigma \mathcal{V}^T. \quad (7)$$

where Σ contains the singular values, ordered as $\sigma_1 > \sigma_2 > \dots > 0$. We consider $\Psi = \mathcal{U}^r \in \mathbb{R}^{N \times r}$, that corresponds to the truncation (r first columns, which has larger singular values than a pre-defined error tolerance ε) with orthogonal matrices $\mathcal{U} \in \mathbb{R}^{N \times r}$ and $\mathcal{V} \in \mathbb{R}^{M \times r}$. Therefore, the RO system of (5) reads

$$[A_{\Delta t}^r + B^r]x_k^r = A_{\Delta t}^r x_{k-1}^r + C_k^r, \quad (8)$$

with $A_{\Delta t}^r = \Psi^T A_{\Delta t} \Psi$, $B^r = \Psi^T B \Psi$ and $C^r = \Psi^T C$ [16].

3.1 Application to an electro-mechanical problem with movement

3.1.1 RO modelling with automatic remeshing technique

In case of automatic remeshing, we transfer results from the source mesh $_{k-1}$ to the new target mesh $_k$ by means of a Galerkin projection, which is optimal in the L_2 -

norm sense [17]. Note that, this projection is limited to the conducting domain, i.e. the plate, as it is only there that we need to compute the time derivative. The number of unknowns per time step t_k varies and the construction of the snapshot matrix S is not straightforward. As the solution at t_k is supported on its own mesh, the snapshot vectors x_k have a different size. They have to be projected to a common basis using a simple linear interpolation technique before being assembled in S and getting the projection operator Ψ . The procedure becomes thus extremely inefficient.

3.1.2 RO modelling with mesh deformation technique

The automatic remeshing task is replaced by a mesh deformation technique, limited to a region around the moving body (see, e.g., the box in Fig. 2). Therefore, in this case, the remeshing is done by deforming the initial mesh, which is generated with the conducting plate placed at, e.g., y_0 (avoiding bad quality elements), see Fig. 2. The mesh elements only inside the sub-domain can be deformed (shrink/expand), see Fig. 3 and the nodes at the boundary of the sub-domain are fixed. The surrounding mesh does not vary. In our test case, we assume a vertical force (neglect the other two components) in (2), therefore, the mesh elements only deform in the vertical direction and the nodes are fixed at the boundary of the sub-domain (not at the axes due to the axisymmetry). The size of the sub-domain ($a \times b$) is determined by the extreme positions of the moving body. In our validation example, the minimum position (3.8 mm) is given by the upper borders of the coils and the maximum position (22.3 mm) could be estimated by means of a circuital model, e.g. [5]. The number of unknowns per time step remains now constant so the construction of matrix S is direct.

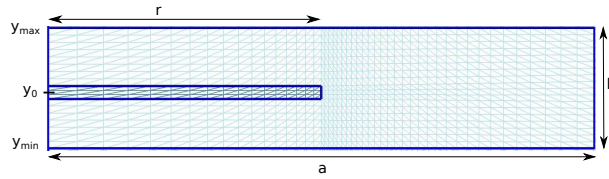


Fig. 2: Sub-domain for deformation: plate position at $y_0 = 12.8$ mm (initial mesh).

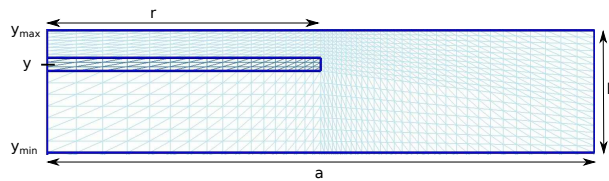


Fig. 3: Sub-domain for deformation: plate position at $y = 20$ mm. Mesh elements under the plate are expanded and above the plate are shrunk.

Algorithm 1: Automatic remeshing

Input : snapshot vectors
 $\{S_c\} \leftarrow \{x_k\} \in \mathbb{R}^{n(k) \times 1}$
time steps
 $\{t_k\}, k \in [1, \dots, K]$
 $A_{\Delta t}, B, C$, tolerance ε
 $m \leq n(k)$ snapshot vectors

Output: displacement y_k

- 1 $y_0 =$ initial position, $\Delta y_0 = 0$
//Time resolution
- 2 **for** $k \leftarrow 1$ **to** K **do**
//Magnetics
 - 3 generate matrices $A_{\Delta t_k}, B_k, C_k$
 - 4 find length of $C_k \in \mathbb{R}^{n(k) \times 1}$
 - 5 $S_p = \mathbf{0} \in \mathbb{R}^{n(k) \times m}$
 - 6 $S_p \leftarrow$ projection of $\{S_c\}$ to $n(k)$
rank subspace
 - 7 SVD of $S_p = \mathcal{U} \Sigma \mathcal{V}^T$
 - 8 $\Psi_k = \mathcal{U}(:, 1 \dots r)$ with r such
that $\sigma(i)/\sigma(1) > \varepsilon, \forall i \in [1 \dots r]$
 $A_{\Delta t_k}^r = \Psi_k^T A_{\Delta t_k} \Psi_k,$
 - 9 $B_k^r = \Psi_k^T B_k \Psi_k,$
 $C_k^r = \Psi_k^T C_k$
- 10 solve
 $(A_{\Delta t_k}^r + B_k^r) x_k^r = C_k^r + A_{\Delta t_k}^r x_{k-1}^r$
- 11 $x_k \approx \Psi_k x_k^r$
- 12 compute force F_k
//Mechanics
- 13 compute displacement y_k
- 14 update $\Delta y_k = y_k - y_{k-1}$
- 15 remesh with y_k
- 16 **end**

Algorithm 2: Mesh deformation

Input : snapshot matrix
 $S = [x_1, \dots, x_m] \in \mathbb{R}^{n \times m},$
 $x_k \in \mathbb{R}^{n \times 1}$
time steps
 $\{t_k\}, k \in [1, \dots, K]$
 $A_{\Delta t}, B, C$, tolerance ε
 $m \leq n$ snapshot vectors

Output: displacement y_k

- 1 $y_0 =$ initial position, $\Delta y_0 = 0$
- 2 get initial mesh
- 3 SVD of $S = \mathcal{U} \Sigma \mathcal{V}^T$
- 4 $\Psi_k = \mathcal{U}(:, 1 \dots r)$ with r such that
 $\sigma(i)/\sigma(1) > \varepsilon, \forall i \in [1 \dots r]$
//Time resolution
- 5 **for** $k \leftarrow 1$ **to** K **do**
//Magnetics
 - 6 generate matrices $A_{\Delta t_k}, B_k, C_k$
 $A_{\Delta t_k}^r = \Psi_k^T A_{\Delta t_k} \Psi_k,$
 - 7 $B_k^r = \Psi_k^T B_k \Psi_k,$
 $C_k^r = \Psi_k^T C_k$
 - 8 solve
 $(A_{\Delta t_k}^r + B_k^r) x_k^r = C_k^r + A_{\Delta t_k}^r x_{k-1}^r$
 - 9 $x_k \approx \Psi_k x_k^r$
 - 10 compute force F_k
//Mechanics
 - 11 compute displacement y_k
 - 12 update $\Delta y_k = y_k - y_{k-1}$
 - 13 deform mesh with y_k
 - 14 **end**

4 Application example

We consider TWP28: an electrodynamic levitation device consisting of a conducting cylindrical aluminium plate ($\sigma = 3.47 \cdot 10^7$ S/m, $m = 0.107$ Kg, $\xi = 1$) above two coaxial exciting coils. The inner and outer coils have 960 and 576 turns respectively. Note that, if we neglect the elastic force, the equilibrium is reached when the F_{em} is

1N. At $t = 0$, the plate rests above the coils at a distance of 3.8 mm. For $t \geq 0$, a time-varying sinusoidal current (20 A, $f = 50$ Hz) is imposed, same amplitude, opposite directions [13]. Assuming a translational movement (no rotation and tilting) we can use an axisymmetric model. A FE model is generated as reference and origin of the RO models. We have time-stepped 50 periods (100 time steps per period and step size 0.2 ms), discretization that ensures accuracy and avoids degenerated mesh elements during deformation.

4.1 RO modelling with automatic remeshing full domain

In case of full domain remeshing, the first 1500 time steps (300 ms) of the simulation, that correspond to the first two peaks (2P) in Fig. 4, are included in the snapshot matrix.

Three POD-based RO models are constructed based on the r number of first singular value modes greater than a prescribed error tolerance ε , that is set manually observing the singular values decay curve of the snapshot matrix (see in Table 1). The smaller the prescribed ε , the bigger the size of the RO model will be (size of $RO3 > RO2 > RO1$).

Table 1: L_2 -relative errors of RO models on levitation height for 2P (automatic remeshing).

RO models	M	ε	rel. error
RO1	1085	10^{-6}	$1.25 \cdot 10^{-1}$
RO2	1403	10^{-11}	$1.03 \cdot 10^{-2}$
RO3	1411	10^{-15}	$2.45 \cdot 10^{-6}$

The displacement and relative error of the full and RO models are shown in Fig. 4. Accurate results have been achieved with the truncated basis models: RO2 and RO3, with fix size per time step $M = 1403$ and 1411 . This approach is completely inefficient, as the maximum number of unknowns we have in the full model is 1552.

4.2 RO modelling with mesh deformation of a sub-domain

The choice of the sub-domain to deform the mesh is a non-trivial task: it should be as small as possible while ensuring a high accuracy. From our reference FE solution [13], by observing the minimum and maximum levitation height of the plate, we fixed the sub-domain size along the y -axis between $y_{min} = 1.3$ mm and $y_{max} = 29.3$ mm, distances measured from the upper border of the coils. The size along the x -axis has a minimum equal to the radius of the plate, i.e. $r = 65$ mm. This value is however not enough due to fringing effects. We have taken different

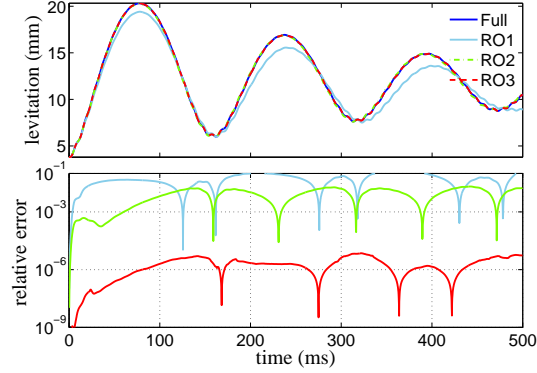


Fig. 4: Displacement (up) and relative error (down) between full and RO models.

size along the x -axis: $1.5r, 2r, 3r$ (97.5, 130 and 195 mm), measured from the axis (Fig. 2). The meshed boxes yield 1921, 1836 and 1780 number of unknowns.

The relative errors in time shown in Table 2 decrease with the increasing sub-domain lengths/box sizes considered. We have therefore chosen to further analyse the RO results obtained with a box length along x of 195 mm ($3r$). The discretization is kept constant for all RO models computation.

Table 2: L_2 -relative errors of RO models on levitation height for 1P (mesh deform).

sub-domain lengths (mm)	$M = 7$	$M = 35$
97.5	$8.24 \cdot 10^{-2}$	$6.14 \cdot 10^{-4}$
130	$5.71 \cdot 10^{-2}$	$1.90 \cdot 10^{-4}$
195	$4.53 \cdot 10^{-3}$	$3.73 \cdot 10^{-5}$

The first 800 time steps (160 ms) of the simulation, that correspond to the first peak (1P), are taken in the snapshot matrix in order to generate the projection basis Ψ . In the snapshot matrix, the most important time step solutions are included, which found as optimum selection for approximating the full solution. Then the basis is truncated as $\Psi = \mathcal{U}^r$ (r first columns) by means of prescribed error tolerance ($\varepsilon = 10^{-5}, 10^{-8}$). The basis are truncated for 1P to get RO models of size $M = 7$ and 35.

From Fig. 5, it can be observed that, RO model already shows very good argument with only $M = 7$ truncated basis, which is generated from the snapshot matrix that incorporates first peak (1P). The accuracy of RO models does not improve significantly with the addition of following transient peaks (2P) into the snapshot matrix, but the accuracy certainly improves with M . Hence, with $M = 35$ the full and RO curves are indistinguishable. The accuracy of the RO models can also be observed from the L_2 -relative errors figure.

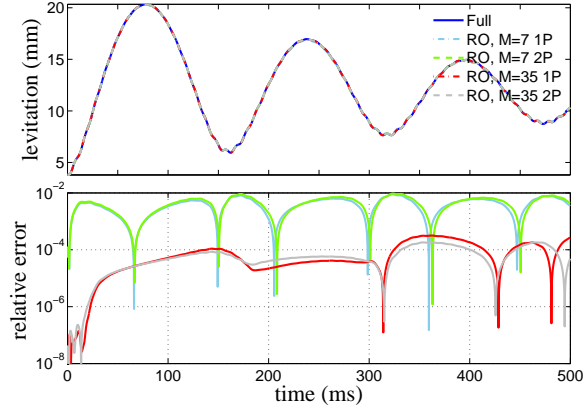


Fig. 5: Displacement (up) and relative error (down) between full and RO models for 195 mm sub-domain length.

With regard to the computation time (5000 time steps), the RO with $M = 7$, can be solved less than an hour, which is 3.5 times faster than the full-domain automatic remeshing approach, where the major time consuming part is to project the Ψ on a same dimensional basis as the system coefficient matrices, to reduce the system in each time step. Be aware that the computation is not optimized, performed on a laptop, (Intel Core i7-4600U CPU at 2.10 GHz) without any parallelization.

5 Conclusion

In this paper, we have proposed two approaches for POD-based RO models to treat a magnetodynamic levitation problem: automatic remeshing and mesh deformation of a sub-domain around a moving body. The RO model is completely inefficient with automatic remeshing technique, as the computational cost is nearly expensive as the classical approach. The approach with sub-domain deformation to limit the influence of the movement on the RO model construction has proved accurate and efficient (low computational cost). We have shown results for three different sub-domain sizes, the bigger the sub-domain the higher the accuracy. Further, computationally efficient RO modelling of such parametric model is ongoing research.

References

1. Sabariego, R., Gyselinck, J., Dular, P., Geuzaine, C., Legros W.: Fast multipole acceleration of the hybrid finite-element/boundary-element analysis of 3-D eddy-current problems. IEEE

- Trans. Magn. vol. 40, no. 2, pp. 1278–1281, (2004).
2. Boualem, B., Piriou, F.: Numerical models for rotor cage induction machines using finite element method. *IEEE Trans. on Magn.*, vol. 34, no. 5, pp. 3202–3205, (1998).
 3. Rapetti, F.: An overlapping mortar element approach to coupled magneto-mechanical problems. *Math. and Comput. in Sim.*, vol. 88, no. 8, pp. 1647–1656, (2010).
 4. Liu, Z., Liu, S., Mohammed, O. A.: A Practical Method for Building the FE-Based Phase Variable Model of Single Phase Transformers for Dynamic Simulations. *IEEE Trans. Magn.*, vol. 43, no. 4, pp. 1761–1764, (2007).
 5. Lee, S. M., Lee, S. H., Choi, H. S., Park, I. H.: Reduced Modeling of Eddy Current-Driven Electromechanical System Using Conductor Segmentation and Circuit Parameters Extracted by FEA. *IEEE Trans. Mag.*, vol. 41, no. 5, pp. 1448–1451, (2005).
 6. Schilders, W.H., Van der Vorst, H.A. and Rommes, J.: *Model order reduction: theory, research aspects and applications*. Springer-Verlag, (2008).
 7. Yue, Y., Feng, L., Meuris, P., Schoenmaker, W., Benner, P.; Application of Krylov-type Parametric Model Order Reduction in Efficient Uncertainty Quantification of Electro-thermal Circuit Models. In *Proc. of the Prog. In Electromag. Res. Symp. (PIERS)*, pp. 379–384, (2015).
 8. Banagaaya, N., Feng, L., Meuris, P., Schoenmaker, W., Benner, P.; Model order reduction of an electro-thermal package model. *IFAC-PapersOnLine*, vol. 48, no. 1, pp. 934–935, (2015).
 9. Alburni, M.N., Rischmuller, V., Fritzsche, T., Lohmann, B.: Model-order reduction of moving nonlinear electromagnetic devices. *IEEE Trans. Mag.*, vol. 44, no. 7, pp. 1822–1829, (2008).
 10. Henneron, T., Clénet, S., Model order reduction applied to the numerical study of electrical motor based on POD method taking into account rotation movement. *Int. J. Numer. Model.*, vol. 27, no. 3, pp. 485–494, (2014).
 11. Sato, T., Sato, Y., Igarashi, H.: Model order reduction for moving objects: fast simulation of vibration energy harvesters. *COMPEL*, vol. 34, no. 5 pp. 1623–1636, (2015).
 12. Schmidhäusler, D., Schöps and Clemens, M.: Linear subspace reduction for quasistatic field simulations to accelerate repeated computations. *IEEE Trans. Magn.*, vol. 50, no. 2, article # 7010304, (2014).
 13. Karl, H., Fetzner, J., Kurz, S., Lehner, G., Rucker, W. M.: Description of TEAM workshop problem 28: An electrodynamic levitation device. In *Proc. of the TEAM Workshop, Graz, Austria*, pp. 48–51, (1997).
 14. Henrotte, F., Nicolet, A., Hedia, H., Genon, A., Legros, W.; Modelling of electromechanical relays taking into account movement and electric circuits. *IEEE Trans. Magn.* vol. 30, no. 5, pp. 3236–3239, (1994).
 15. Sato, Y., Igarashi, H.: Model reduction of three-dimensional eddy current problems based on the method of snapshots. *IEEE Trans. Magn.*, vol. 49, no. 5, pp. 1697–1700, (2013).
 16. Hasan, MD R., Sabariego, R. V., Geuzaine, C., Paquay, Y.; Proper orthogonal decomposition versus Krylov subspace methods in reduced-order energy-converter models. In *Proc. of IEEE Inter. Ener. Conf.*, pp. 1–6, (2016).
 17. Parent, G., Dular, P., Ducreux, J.P. and Piriou, F.; Using a Galerkin projection method for coupled problems. *IEEE Trans. Magn.*, vol. 44, no. 6, pp. 830–833, (2008).